

# Oxygen at Nanomolar Levels Reversibly Suppresses Process Rates and Gene Expression in Anammox and Denitrification in the Oxygen Minimum Zone off Northern Chile

Tage Dalsgaard,<sup>a,b</sup> Frank J. Stewart,<sup>c</sup> Bo Thamdrup,<sup>d</sup> Loreto De Brabandere,<sup>d</sup> Niels Peter Revsbech,<sup>e</sup> Osvaldo Ulloa,<sup>f</sup> Don E. Canfield,<sup>d</sup> Edward F. DeLong<sup>g,h</sup>

Department of Bioscience, Aarhus University, Silkeborg, Denmark<sup>a</sup>; Arctic Research Centre, Aarhus University, Aarhus, Denmark<sup>b</sup>; School of Biology, Georgia Institute of Technology, Atlanta, Georgia, USA<sup>c</sup>; Department of Biology and Nordic Center for Earth Evolution (NordCEE), University of Southern Denmark, Odense, Denmark<sup>d</sup>; Department of Bioscience, Aarhus University, Aarhus, Denmark<sup>e</sup>; Departamento de Oceanografía & Instituto Mileno de Oceanografía, Universidad de Concepción, Concepción, Chile<sup>f</sup>; Department of Civil and Environmental Engineering, Massachusetts Institute of Technology, Cambridge, Massachusetts, USA<sup>g</sup>; Department of Oceanography, University of Hawai'i, Mānoa, Hawai'i, USA<sup>h</sup>

**ABSTRACT** A major percentage (20 to 40%) of global marine fixed-nitrogen loss occurs in oxygen minimum zones (OMZs). Concentrations of O<sub>2</sub> and the sensitivity of the anaerobic N<sub>2</sub>-producing processes of anammox and denitrification determine where this loss occurs. We studied experimentally how O<sub>2</sub> at nanomolar levels affects anammox and denitrification rates and the transcription of nitrogen cycle genes in the anoxic OMZ off Chile. Rates of anammox and denitrification were reversibly suppressed, most likely at the enzyme level. Fifty percent inhibition of N<sub>2</sub> and N<sub>2</sub>O production by denitrification was achieved at 205 and 297 nM O<sub>2</sub>, respectively, whereas anammox was 50% inhibited at 886 nM O<sub>2</sub>. Coupled metatranscriptomic analysis revealed that transcripts encoding nitrous oxide reductase (*nosZ*), nitrite reductase (*nirS*), and nitric oxide reductase (*norB*) decreased in relative abundance above 200 nM O<sub>2</sub>. This O<sub>2</sub> concentration did not suppress the transcription of other dissimilatory nitrogen cycle genes, including nitrate reductase (*narG*), hydrazine oxidoreductase (*hzo*), and nitrite reductase (*nirK*). However, taxonomic characterization of transcripts suggested inhibition of *narG* transcription in gammaproteobacteria, whereas the transcription of anammox *narG*, whose gene product is likely used to oxidatively replenish electrons for carbon fixation, was not inhibited. The taxonomic composition of transcripts differed among denitrification enzymes, suggesting that distinct groups of microorganisms mediate different steps of denitrification. Sulfide addition (1 μM) did not affect anammox or O<sub>2</sub> inhibition kinetics but strongly stimulated N<sub>2</sub>O production by denitrification. These results identify new O<sub>2</sub> thresholds for delimiting marine nitrogen loss and highlight the utility of integrating biogeochemical and metatranscriptomic analyses.

**IMPORTANCE** The removal of fixed nitrogen via anammox and denitrification associated with low O<sub>2</sub> concentrations in oceanic oxygen minimum zones (OMZ) is a major sink in oceanic N budgets, yet the sensitivity and dynamics of these processes with respect to O<sub>2</sub> are poorly known. The present study elucidated how nanomolar O<sub>2</sub> concentrations affected nitrogen removal rates and expression of key nitrogen cycle genes in water from the eastern South Pacific OMZ, applying state-of-the-art <sup>15</sup>N techniques and metatranscriptomics. Rates of both denitrification and anammox responded rapidly and reversibly to changes in O<sub>2</sub>, but denitrification was more O<sub>2</sub> sensitive than anammox. The transcription of key nitrogen cycle genes did not respond as clearly to O<sub>2</sub>, although expression of some of these genes decreased. Quantifying O<sub>2</sub> sensitivity of these processes is essential for predicting through which pathways and in which environments, from wastewater treatment to the open oceans, nitrogen removal may occur.

Received 17 September 2014 Accepted 23 September 2014 Published 28 October 2014

**Citation** Dalsgaard T, Stewart FJ, Thamdrup B, De Brabandere L, Revsbech NP, Ulloa O, Canfield DE, DeLong EF. 2014. Oxygen at nanomolar levels reversibly suppresses process rates and gene expression in anammox and denitrification in the oxygen minimum zone off Northern Chile. *mBio* 5(6):e01966-14. doi:10.1128/mBio.01966-14.

**Editor** Douglas G. Capone, University of Southern California

**Copyright** © 2014 Dalsgaard et al. This is an open-access article distributed under the terms of the [Creative Commons Attribution-Noncommercial-ShareAlike 3.0 Unported license](https://creativecommons.org/licenses/by-nc-sa/4.0/), which permits unrestricted noncommercial use, distribution, and reproduction in any medium, provided the original author and source are credited.

Address correspondence to Tage Dalsgaard, tda@dmu.dk.

This article is a direct contribution from a Fellow of the American Academy of Microbiology.

Oxygen (O<sub>2</sub>) plays a key role in regulating the major biogeochemical cycles in the marine environment (1). The present-day ocean is generally well oxygenated, but in some environments, the demand for O<sub>2</sub> exceeds the rate of supply, causing low-O<sub>2</sub> environments to develop. This is the case in oxygen minimum zones (OMZ) (2–6) and sediments (7), which may be anoxic or at least have O<sub>2</sub> concentrations below the detection limits of the

methods used for analysis of O<sub>2</sub>. In these environments, a suite of anaerobic processes may occur that utilize nitrate (NO<sub>3</sub><sup>-</sup>), nitrite (NO<sub>2</sub><sup>-</sup>), sulfate (SO<sub>4</sub><sup>2-</sup>), and metal oxides as terminal electron acceptors (8). In OMZs, NO<sub>3</sub><sup>-</sup> and NO<sub>2</sub><sup>-</sup> concentrations are generally high and nitrogen oxyanions are believed to be the main terminal electron acceptors (9). It has also recently been shown that a cryptic sulfur cycle operates in the eastern South Pacific

OMZ, in which sulfate reduction oxidizes organic matter and produces sulfide. However, sulfide does not accumulate, presumably because it is immediately oxidized by  $\text{NO}_3^-$ - and  $\text{NO}_2^-$ -reducing chemoautotrophic microbes (10). The OMZs play an important role in the marine nitrogen cycle, and the ocean's three major OMZs (eastern South Pacific, eastern North Pacific, and Arabian Sea) are estimated to harbor 20 to 40% of the oceanic reactive nitrogen loss (11, 12). The conversion of reactive nitrogen to  $\text{N}_2$  occurs through microbial denitrification and anammox, but the relative importance of these sinks is debated (13–15), and the final conversion to  $\text{N}_2$  appears to proceed in close interaction with other nitrogen, carbon, and sulfur transformations, which together drive dissimilatory reduction of  $\text{NO}_3^-$  to  $\text{NO}_2^-$  and of  $\text{NO}_2^-$  to ammonium ( $\text{NH}_4^+$ ), as well as aerobic oxidation of  $\text{NH}_4^+$  and  $\text{NO}_2^-$  (e.g., see references 15 and 16).

The distribution of  $\text{O}_2$  in OMZs and its effect on both aerobic and anaerobic nitrogen transformations is of central importance for understanding the role of OMZs in the marine nitrogen cycle and predicting changes in response to environmental forcing. Recent results obtained using highly sensitive switchable trace oxygen (STOX) sensors (17, 18) indicate that the core of the OMZs is functionally anoxic, with  $\text{O}_2$  levels below the detection limit of a few nanomolar (2), but with episodic intrusions of more oxygenated waters (6, 19). At the boundaries of the core and after mixing events,  $\text{O}_2$  is present at low concentrations, potentially allowing interactions between aerobic and anaerobic processes (e.g., see reference 20).  $\text{N}_2$  production is particularly intense in these transition zones (14, 16), which emphasizes the need for quantification of the  $\text{O}_2$  sensitivity and dynamic response of the individual processes. Existing estimates of the  $\text{O}_2$  tolerance of denitrification and anammox differ greatly. Experimental studies with oxygen addition have found anammox in OMZs and the Black Sea to require 2 to 16  $\mu\text{M}$   $\text{O}_2$  for 50% inhibition (21–23), while the abrupt increase in anammox activity at the upper oxic-anoxic interface of the OMZ off Peru and Chile suggests a much greater sensitivity to oxygen exposure *in situ* (14). A single experimental study of the oxygen sensitivity of denitrification in an OMZ found the process to be completely inhibited at 3  $\mu\text{M}$   $\text{O}_2$ , while anammox still proceeded at low rates (23). This could indicate, as suggested earlier (24), that denitrification in OMZs may be more sensitive than anammox to  $\text{O}_2$ , but whether this is more general remains to be experimentally verified, and denitrification is often assumed to be active at micromolar  $\text{O}_2$  levels (e.g., see references 25 and 26). The assumed  $\text{O}_2$  sensitivity of these processes plays a vital role when the volume of water in the oceans that can be assumed to participate in  $\text{N}_2$  production is estimated, and this volume may vary greatly depending on which threshold is chosen; assuming inhibition at nanomolar  $\text{O}_2$  concentrations would result in a significantly smaller zone of  $\text{N}_2$  production than if inhibition is assumed to occur up to 20  $\mu\text{M}$   $\text{O}_2$  (26).

Rates of nitrogen transformation in OMZs are determined experimentally in batch incubations with  $^{15}\text{N}$ -labeled compounds (15, 27). These measurements reflect the metabolism of the microbial community as a whole and can reveal the bulk kinetics of the processes with respect to environmental parameters such as  $\text{O}_2$ . Such kinetics represent the composite of the responses of different types of organisms with distinct physiologies. In another approach, patterns of gene transcription can be analyzed to estimate the activities of different functional pathways and taxonomic members of the microbial community, potentially providing in-

sight into microbial  $\text{O}_2$  sensitivity of individual clades. Gene expression over vertical  $\text{O}_2$  gradients in OMZs has been assessed via quantitative PCR (qPCR) using reverse-transcribed RNA and gene-specific primers (e.g., see reference 15). This approach typically targets only a subset of metabolic processes and is subject to biases due to primer-template specificity, particularly in environments with high numbers of uncharacterized taxa. Alternatively, high-throughput sequencing and analysis of community cDNA (metatranscriptomics) can identify coexpression patterns of thousands of genes from diverse community members without requiring *a priori* knowledge of sequence identity (28). However, metatranscriptomics typically does not yield absolute measurements of transcript abundance and, depending on sequencing depth, may not detect subtle transcriptional shifts in low-frequency taxa (29). Determining whether metatranscriptome patterns can be proxies for biogeochemical activity requires experiments that couple community RNA sequencing with metabolic rate measurements. Few such studies have been conducted for natural microbial communities, and no studies have examined potential linkages between community transcription and metabolic rates at the nanomolar  $\text{O}_2$  concentrations predicted for the Eastern Pacific OMZs. This is due in part to the challenge of sampling anoxic water columns without concurrent changes in community expression and  $\text{O}_2$  contamination (28, 30).

This challenge can be met by studying natural communities in microcosm (bioreactor) experiments that combine time series rate measurements, RNA collection, and high-sensitivity control of dissolved- $\text{O}_2$  levels, although  $\text{O}_2$  contamination during experimentation is almost inevitable (31). In the present study, we performed  $\text{O}_2$  manipulation experiments in bioreactors. Rates of anammox and denitrification were quantified over variable oxygen treatments, and the expression of key N cycle genes (Fig. 1) at the endpoint of each experiment was analyzed using metatranscriptomics. Each bioreactor was equipped with a STOX sensor, allowing us to directly couple molecular and biogeochemical rate measurements with the precise monitoring of  $\text{O}_2$  at the nanomolar concentration range reflective of the *in situ* OMZ environment. Although enclosure in bioreactors has been shown to alter the metatranscriptional profile of some OMZ community members (i.e., bottle effects) (32), comparisons between bioreactors with contrasting oxygen treatments can help identify gene expression patterns suggestive of differential oxygen sensitivity.

## RESULTS

**Concentrations of  $\text{O}_2$  and  $\text{H}_2\text{S}$ .** Oxygen concentrations were below the detection limit in the OMZ source water, but water sampling using the pump profiling system (PPS) introduced minor amounts of  $\text{O}_2$  contamination into the bioreactors. The  $\text{O}_2$  concentration in the water leaving the hose of the PPS was as low as 20 nM (10), but  $\text{O}_2$  levels were always higher when measured inside the reactors placed in the water bath in the lab (designated “initial” in Table 1).  $\text{O}_2$  contamination was reduced from the first to the third experiment, with initial concentrations exceeding 100 nM in four reactors in experiment 1, in two reactors in experiment 2, and in none of the reactors in experiment 3. All reactors were sparged with helium within the first few hours after arriving in the lab, which brought the  $\text{O}_2$  concentrations to between undetectable and ca. 20 nM. The average and maximum  $\text{O}_2$  concentrations during the first and second halves of the experiments are listed in Table 1. The discrete additions of  $\text{O}_2$  during the experi-

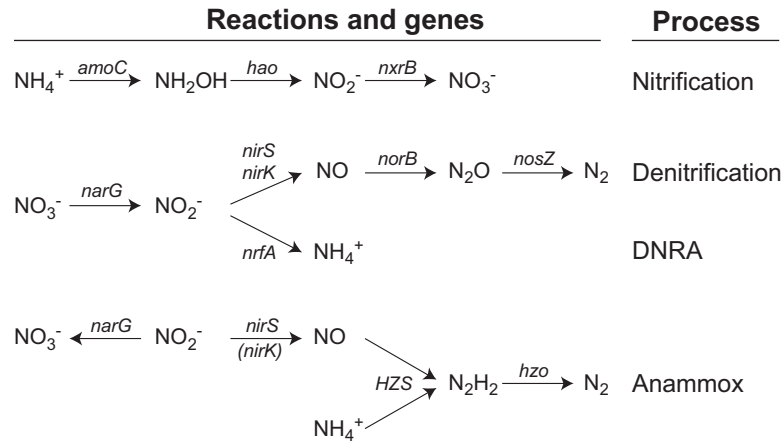


**FIG 1** Overview of the genes and processes discussed in the present study based on the work of van de Vossenberg et al. (36) and Zumft (70). Genes: *amoC*, ammonia monooxygenase (ammonia oxidation); *hao*, hydroxylamine oxidoreductase (ammonia oxidation); *nxrB*, nitrite oxidoreductase (nitrite oxidation); *narG*, nitrate reductase (nitrate reduction); *nirK*, nitrite reductase (nitrite reduction); *nirS*, nitrite reductase (nitrite reduction, putatively more common in anammox, though some have *nirK*); *nrfA*, nitrite reductase (putatively more common in DNRA); *norB*, nitric oxide reductase (nitric oxide reduction); *nosZ*, nitrous oxide reductase (nitrous oxide reduction); *HZS*, hydrazine synthase (anammox; HZS indicates the gene cluster containing *hzsA*, *hzsB*, and *hzsC*); *hzo*, hydrazine oxidoreductase (anammox). Note that the *hao* gene has not been found in the nitrifying archaea (71).

ments resulted in fluctuating  $\text{O}_2$  concentrations, with the worst case shown in Fig. 2B (Table 1). Leakage into the reactors increased  $\text{O}_2$  concentrations during the first half of the incubation to an average of 20 to 90 nM in experiment 1 and 4 to 37 nM in

experiments 2 and 3 (Table 1). The source of this leakage was probably release of  $\text{O}_2$  from the O rings and the edge of the PVC (polyvinyl chloride) plunger, which were the only nonglass parts in contact with the water, similar to the release of  $\text{O}_2$  from rubber

**TABLE 1** Overview of experiments

Experiment	$\text{O}_2$ treatment <sup>a</sup>	Reactor	$\text{H}_2\text{S}$ ( $\mu\text{M}$ ) <sup>b</sup>	$\text{O}_2$ concn (nM) <sup>c</sup>						Gene expression analyzed	
				Initial <sup>d</sup>	First half			Second half			
					Avg	SE	Max <sup>e</sup>	Avg	SE	Max <sup>e</sup>	
1A	HL	1		145	2,737.8	795.6	3,671.8	13.1	5.4	21.5	
1B	LH	2		94	39.9	6.8	56.6	200.3	47.1	275.3	
1B	LH	3		125	91.9	9.0	106.5	201.4	54.3	288.9	x
1C	LH	4		377	88.6	7.6	105.6	558.3	146.1	819.4	x
1C	LH	5		45	28.3	2.2	32.5	486.7	71.6	607.8	
1D	LH	6		78	51.0	2.3	56.8	1,766.2	39.7	1,835.4	x
1E	L	7		54	21.2	11.3	56.9	34.2	2.9	39.4	x
1E	L	8		222	41.8	6.9	57.0	72.5	76.7	205.4	x
2A	HL	1		25	1,830.1	148.0	2,105.5	7.1	2.8	16.4	x
2A	HL	6		62	1,781.9	182.3	2,183.7	2.6	4.1	39.4	
2B	H	4		161	1,680.4	283.0	2,176.4	1,630.1	179.0	1,935.2	
2B	H	8		28	1,806.7	198.7	2,138.3	1,723.5	236.9	2,106.3	x
2C	LH	3	1,670		32.3	5.7	43.9	1,537.2	416.9	2,233.4	x
2C	LH	7		19	16.8	3.4	26.9	1,756.2	149.8	2,056.2	
2D	L	2		8	19.4	5.4	29.6	10.5	6.1	57.1	x
2D	L	5		41	11.8	3.1	17.2	7.1	1.9	11.9	x
3A	LH	5	1.1	57	15.0	11.9	99.8	393.7	128.4	706.3	
3A	LH	6	1.0	44	7.7	5.8	21.7	391.2	50.9	479.2	
3B	LH	3	1.2	38	37.3	9.5	49.8	1,789.9	389.2	2,655.2	
3C	L	7	1.3	45	13.4	13.2	43.1	7.8	7.8	34.9	
3C	L	8	1.4	36	4.1	4.1	20.5	3.5	1.8	8.5	
3D	L	1	0.0	68	17.8	3.3	26.6	9.0	3.5	19.8	
3D	L	2	0.0	34	14.8	2.7	19.1	7.0	2.5	12.2	

<sup>a</sup> L, continuously low; H, continuously high; LH, low during the first half and high during the last half; HL, high during the first half and low during the last half.

<sup>b</sup> Average  $\text{H}_2\text{S}$  (sum of  $\text{H}_2\text{S}$ ,  $\text{HS}^-$ , and  $\text{S}^{2-}$ ) concentrations during the incubations (experiment 3 only).

<sup>c</sup> SE, standard error of the average.

<sup>d</sup> First recorded concentration when the reactor was fitted with a STOX sensor.

<sup>e</sup> Highest recorded  $\text{O}_2$  concentrations after the initial helium gassing.

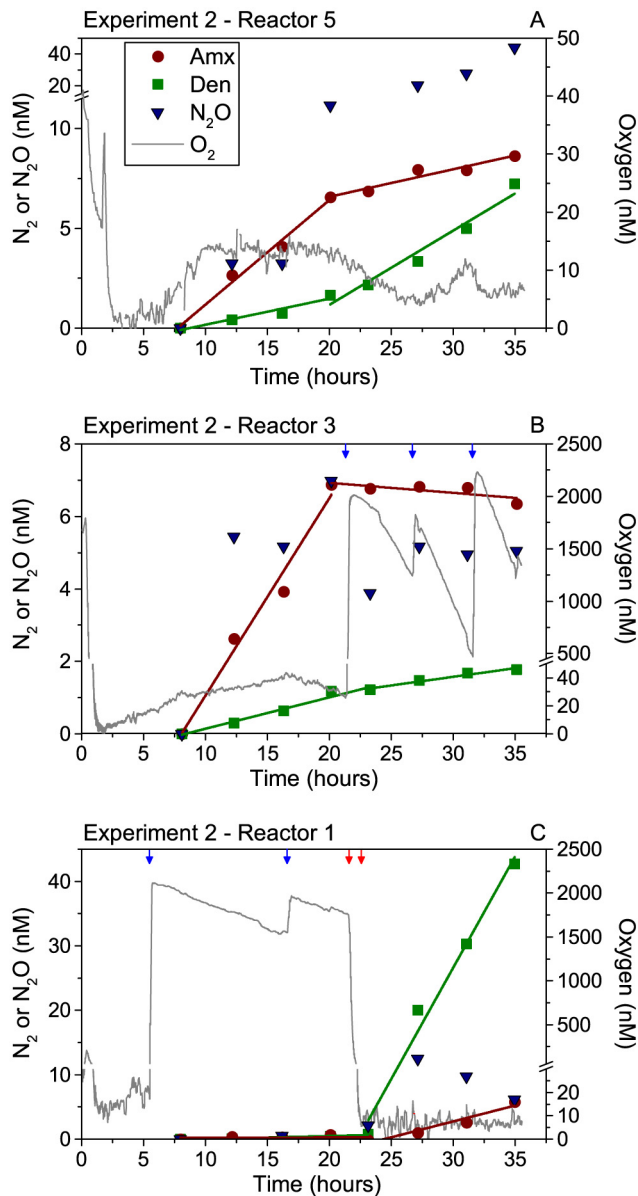


**FIG 2**  $N_2$  produced by anammox and denitrification,  $N_2O$  produced by denitrification, and  $O_2$  concentrations in reactor experiments at station 5.  $^{15}NO_2^-$  was added 20 to 30 min before the first sampling for  $N_2$  and  $N_2O$ . Air-saturated water was injected at 21.6, 26.8, and 31.7 h (B) and at 5.7 and 16.7 h (C) (blue arrows). He sparging took place between 21.7 and 22.6 h (C; red arrows). Regression lines indicate the linear changes in  $N_2$  concentrations over the first and second halves of the incubation in the no-oxygen amendment incubation (A) and before and after the increase (B) and decrease (C) in  $O_2$  concentration.

septa demonstrated in glass vials (31). This leakage was not constant, and it was thus not possible to estimate the  $O_2$  respiration in the water accurately.

**Production of  $N_2$  and  $N_2O$ .** In all control experiments with low  $O_2$  throughout, the rate of denitrification increased from the first to the second half of the incubation, whereas the anammox rate decreased (e.g., slope of regression lines in Fig. 2A). The changes were gradual but could be approximated by two linear regressions. In all cases when  $O_2$  concentrations were raised, there

was an immediate decrease in the production rates of  $N_2$  by both processes (e.g., Fig. 2B). Conversely, process rates increased when  $O_2$  concentrations were lowered to levels similar to those in the control incubations (Fig. 2C). This change was evident immediately after the  $O_2$  level reached the low nM range, but the processes could have accelerated even earlier, because the 1-h sparging performed to remove  $O_2$  would also have removed any  $^{15}N$ -labeled  $N_2$  formed during this period. Denitrification produced  $N_2O$  at rates similar to the  $N_2$  production rates, although with a higher variation. Nitrous oxide was both produced and consumed, which in some cases resulted in a net decrease in  $N_2O$  concentration, e.g., as seen in the experiment depicted in Fig. 2C. The effects of  $O_2$  on production of  $N_2$  and  $N_2O$  by denitrification were similar, with  $N_2O$  production accelerating through the incubation in the low- $O_2$  controls, being inhibited by amendment of  $O_2$  (e.g., Fig. 2B), and increasing very rapidly after removal of  $O_2$  (e.g., Fig. 2C). The variation in initial rates of anammox and denitrification in the controls was relatively small between the three experiments, with anammox varying from 0.52 to 0.74 nM  $N_2$  h $^{-1}$  and  $N_2$  and  $N_2 + N_2O$  production by denitrification varying from 0.16 to 0.34 and 0.96 to 1.38 nM  $N_2$  h $^{-1}$ , respectively (Table 2).

**Inhibition kinetics.** The rates of anammox and denitrification from the reactors in which the  $O_2$  concentration was raised halfway through the incubation, and from the control reactors, were normalized (equation 4) and combined to estimate the inhibition of these processes by  $O_2$  (Fig. 3). Assuming an exponential attenuation of rates (equation 5), the  $O_2$  concentration resulting in a 50% inhibition of the process ( $C_{50}$ ) was calculated for each of the four processes:  $N_2$  production by anammox and  $N_2$ ,  $N_2O$ , and  $N_2 + N_2O$  production by denitrification (Table 3). Denitrification was much more sensitive than anammox to  $O_2$ , being 50% inhibited at 200 to 300 nM  $O_2$ , whereas anammox first reached 50% inhibition at approximately 900 nM. The presence of sulfide in experiment 3 apparently did not affect the  $O_2$  inhibition kinetics, and data from all three experiments are included in the analysis (Fig. 3).

**Effects of sulfide.** Addition of 1  $\mu$ M sulfide had no apparent effect on anammox rates, which decreased 30% in the absence and 22% in the presence of sulfide from the first to the second half of the experiment (Fig. 4; decreases in anammox rates between the first and second halves of the experiment and between the presence and absence of sulfide were not statistically significant). Denitrification, on the other hand, was strongly stimulated by sulfide. In the absence of sulfide,  $N_2$  and  $N_2O$  production increased  $\leq 2$ -fold from the first to the second half of the experiment, whereas in the presence of sulfide, the production of these gases increased 4.5- and 6.1-fold, respectively.

**Gene expression.** Associations between oxygen treatments and metatranscriptional profiles suggest differential oxygen sensitivity among key pathways of dissimilatory nitrogen metabolism (Fig. 5 and 6). Because we were unable to sequence replicate reactors for all treatments (Table 1), we cannot statistically confirm the variation between reactor treatments. Nonetheless, several trends in N cycle gene transcript abundance are apparent from Fig. 5 and 6. Compared to treatments with low  $O_2$  throughout or in the second half of the experiment (L and HL in Fig. 5),  $O_2$  addition in experiments 1 and 2 was associated with reductions in the relative abundance of transcripts encoding *nirS*-type nitrite reductase, nitric oxide reductase (*norB*), and nitrous oxide reductase (*nosZ*) (Fig. 5). The suppressive effect of  $O_2$  exposure on *nirS*,

TABLE 2 Rates of N<sub>2</sub> production<sup>a</sup>

Station	Depth (m)	Date	Expt	Rate (nM N <sub>2</sub> h <sup>-1</sup> ) <sup>b</sup>						Relative anammox (%) <sup>c</sup>		Oxygen concn (nM)	
				D (N <sub>2</sub> )		D (total)		A (N <sub>2</sub> )		N <sub>2</sub>	Total	Avg	SE
				Avg	SE	Avg	SE	Avg	SE				
3	75	12 Jan 2010	1	0.34	0.17	1.38	0.83	0.74	0.24	68	35	31.48	10.3
5	86	14 Jan 2010	2	0.16	0.03	1.16	0.20	0.59	0.07	78	34	15.63	3.72
3	82	16 Jan 2010	3	0.25	0.16	0.96	0.36	0.52	0.12	67	35	16.33	1.50

<sup>a</sup> Data are for the first half of the control incubations, where O<sub>2</sub> concentrations were kept as low as possible. All values are means of data from two reactors.

<sup>b</sup> D (N<sub>2</sub>), N<sub>2</sub> production by denitrification; D (total), N<sub>2</sub> + N<sub>2</sub>O production by denitrification; A (N<sub>2</sub>), anammox.

<sup>c</sup> Relative importance of anammox for N<sub>2</sub> production (N<sub>2</sub>) and for N<sub>2</sub> + N<sub>2</sub>O production (total).

*norB*, and *nosZ* transcription was relatively consistent in both low (~200 nM) and high (~1,700 nM) O<sub>2</sub> amendments relative to the controls (Fig. 5, experiment 1). In contrast to these transcript patterns and to rate measurements showing inhibition of anammox and denitrification following O<sub>2</sub> addition, O<sub>2</sub> amendment caused only minor or inconsistent shifts in the abundances of transcripts for dissimilatory nitrate reductase (*narG*) and the hydrazine oxidoreductase (*hzo*) associated with anammox. A dependence on O<sub>2</sub> was also not evident for the alternative copper-containing nitrite reductase (*nirK*) or for the sparingly expressed *nrfa*, associated with dissimilatory nitrite reduction to ammonium (DNRA). Of the enzymes associated with aerobic nitrification, nitrite oxidoreductase (*nxrB*) showed no clear trend in gene expression, while the expression of ammonium monooxygenase (*amoC*) genes from ammonium oxidizers was higher in the O<sub>2</sub>-amended microcosms. (Details on gene transcription in the source water microbial community and on the response of other

genes to low-O<sub>2</sub> treatment can be found in the work of Stewart et al. [32])

BLAST analysis of protein-coding transcripts identified a taxonomically diverse assemblage of microorganisms mediating OMZ nitrogen cycling with more than 20 higher-level taxa represented (Fig. 6). Denitrification genes (*narG*, *nirK*, *nirS*, *norB*, and *nosZ*) were affiliated with a broad range of taxa, and taxonomic composition was highly variable among these genes. For example, *nirS* was mainly expressed by *Gammaproteobacteria* while the expression of *nosZ* was more evenly distributed between *Bacteroidetes/Chlorobi*, *Gammaproteobacteria*, and unidentified organisms. Groups making minor contributions also differed markedly between the two genes. This pattern is consistent with denitrification being the result of individual processes catalyzed by different groups of microorganisms. However, a proportion of these transcripts encode enzymes not involved in classical denitrification. For example, a large part (6 to 52%) of *norB* sequences were most

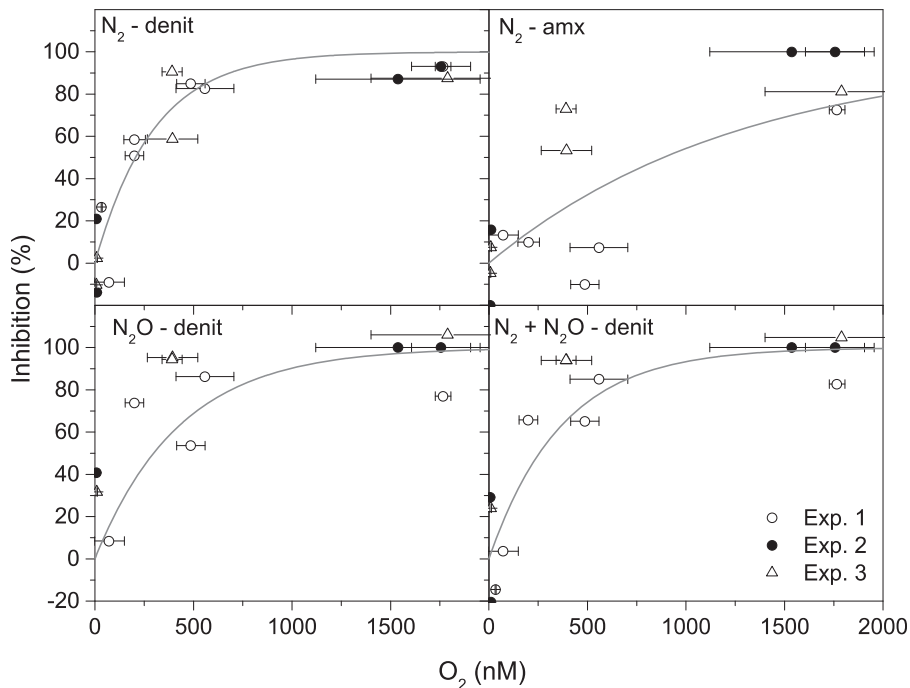


FIG 3 Inhibition of denitrification (N<sub>2</sub>, N<sub>2</sub>O, and N<sub>2</sub> + N<sub>2</sub>O production) and anammox (N<sub>2</sub> production) by O<sub>2</sub> in experiments where O<sub>2</sub> concentration was increased after ca. 20 h. Inhibition was estimated by comparing the rates from before and after O<sub>2</sub> amendment in each individual bioreactor. Error bars show the standard deviations of the average O<sub>2</sub> concentrations for the period after O<sub>2</sub> amendment until the end of the experiment. An exponential-type inhibition kinetics was fitted to the data, as indicated by the lines. See Table 3 for the regression details and results.

**TABLE 3** Parameters for the fit of an exponential-type inhibition kinetics to the measured inhibition by O<sub>2</sub> of denitrification and anammox<sup>a</sup>

Process	C <sub>50</sub> (nM) <sup>b</sup>	R <sup>2</sup>	k
Denitrification			
N <sub>2</sub>	205 (±34)	0.8818	0.00337
N <sub>2</sub> O	297 (±139)	0.5557	0.00233
Total	255 (±88)	0.6968	0.00271
Anammox	886 (±418)	0.4542	0.00078

<sup>a</sup> Data were fitted to the following exponential function: inhibition (%) = 1 - e<sup>-k × C</sup>, applying the Levenberg-Marquardt algorithm (Origin 9.0; OriginLab, MA), where A is the variable coefficient given in Table 2 and C is the oxygen concentration.

<sup>b</sup> O<sub>2</sub> concentration at which 50% inhibition was obtained. Standard errors are in parentheses.

closely related to the quinol-oxidizing variant (qNor) of “*Candidatus* Methyloirabilis oxyfera” (CBE69496.1 and CBE69502.1), a member of the NC10 candidate division enriched from sediment. In this organism, the Nor enzyme may act as a dismutase to convert nitric oxide into dinitrogen and O<sub>2</sub>, with the latter then being used to oxidize methane under anaerobic conditions (33, 34).

Several genes in Fig. 5 and 6 were most closely related to those of known anammox bacteria. The vast majority of *hzo* sequences were either most similar to *hzo* of the marine planctomycete “*Candidatus* Scalindua profunda” or to genes annotated as “uncultured ammonia-oxidizing bacteria” (e.g., accession no. AEP17466 in the NCBI database), labeled as “planctomycetes” and “unknown” in Fig. 6, respectively. In addition, the majority (53 to 88%) of *narG* sequences were most closely related to *narG* of either “*Ca. Scalindua*” or the freshwater anammox bacterium “*Candidatus* Kueneia stuttgartiensis.” It is hypothesized that in anammox bacteria, *narG* acts in reverse as a nitrite oxidoreductase, oxidizing NO<sub>2</sub><sup>-</sup> to NO<sub>3</sub><sup>-</sup> to fuel carbon fixation (35). “*Ca. Scalindua*”-like *nirS* transcripts were also detected, accounting for 2 to 42% of the total *nirS* signal (“planctomycetes” in Fig. 6). However, the relative abun-

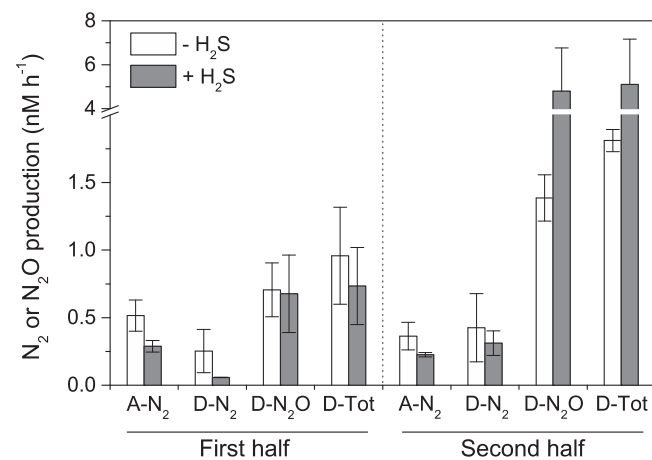


**FIG 4** Rates of anammox and denitrification during the first and second half of experiment 3 (reactors 1, 2, 7, and 8) without O<sub>2</sub> amendment, with and without the amendment of ca. 1 μM H<sub>2</sub>S (actual concentrations are shown in Table 1). A-N<sub>2</sub> is N<sub>2</sub> production by anammox. D-N<sub>2</sub>, D-N<sub>2</sub>O, and D-Tot represent N<sub>2</sub> and N<sub>2</sub>O production by denitrification and total denitrification, respectively. Each column represents the average from two experiments with four or five time points for the rate estimates.

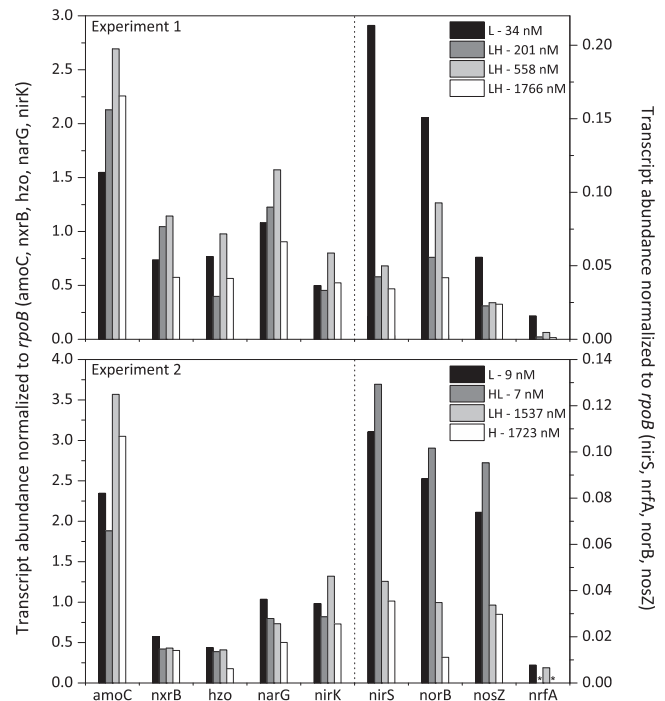


**FIG 5** Relative abundance of reads matching key dissimilatory nitrogen metabolism genes in bioreactor experiments. Transcript abundance is calculated as read count per gene per kilobase of gene length and then normalized as a proportion of the abundance of transcripts matching *rpoB* (see the text). O<sub>2</sub> treatments were continuously low (L), continuously high (H), low during the first half and high during the last half of the incubation (LH), and high during the first half and low during the last half (LH); the average oxygen concentration for the last half of the incubation is indicated. Data for continuously low O<sub>2</sub> concentration is the average for two reactors. Bars to the left of the dotted line scale with the left y axis, and bars to the right with the right y axis. Genes are as in Fig. 1. \*, below detection limit.

dance of these transcripts was an order of magnitude lower than that of “*Ca. Scalindua*” *hzo* and *narG*, which showed similar abundances. Unlike the *nirS* transcription pattern as a whole, “*Ca. Scalindua*”-like *nirS* transcripts did not show consistent patterns of change in response to O<sub>2</sub> amendment; however, the low abundances of these transcripts may have prevented the detection of clear patterns. “*Ca. Scalindua*”-like nitric oxide reductase (*norB*) sequences were also present, but at low abundances comparable to those of “*Ca. Scalindua*” *nirS*. The “*Ca. Scalindua*” *norB* sequences (Fig. 6) were most closely related to a gene encoding a quinol-oxidizing NO reductase (qNor) (gene scal02135). In this bacterium, *norB* may act not in energy metabolism but instead to relieve nitric oxide stress (36), as has been observed for the qNor gene in pathogenic bacteria, though this hypothesis has not yet been confirmed for anammox bacteria. Together, these data highlight variable expression levels among key anammox genes but an overall minor transcriptional response of these genes to O<sub>2</sub> fluctuation over the concentration range and time periods examined here. This pattern is in contrast to the clear inhibition of anammox rates following O<sub>2</sub> addition (Fig. 2).

## DISCUSSION

The effects of O<sub>2</sub> manipulations in coupled measurements of anammox and denitrification rates and community gene transcription were observed for the first time under controlled O<sub>2</sub> condi-

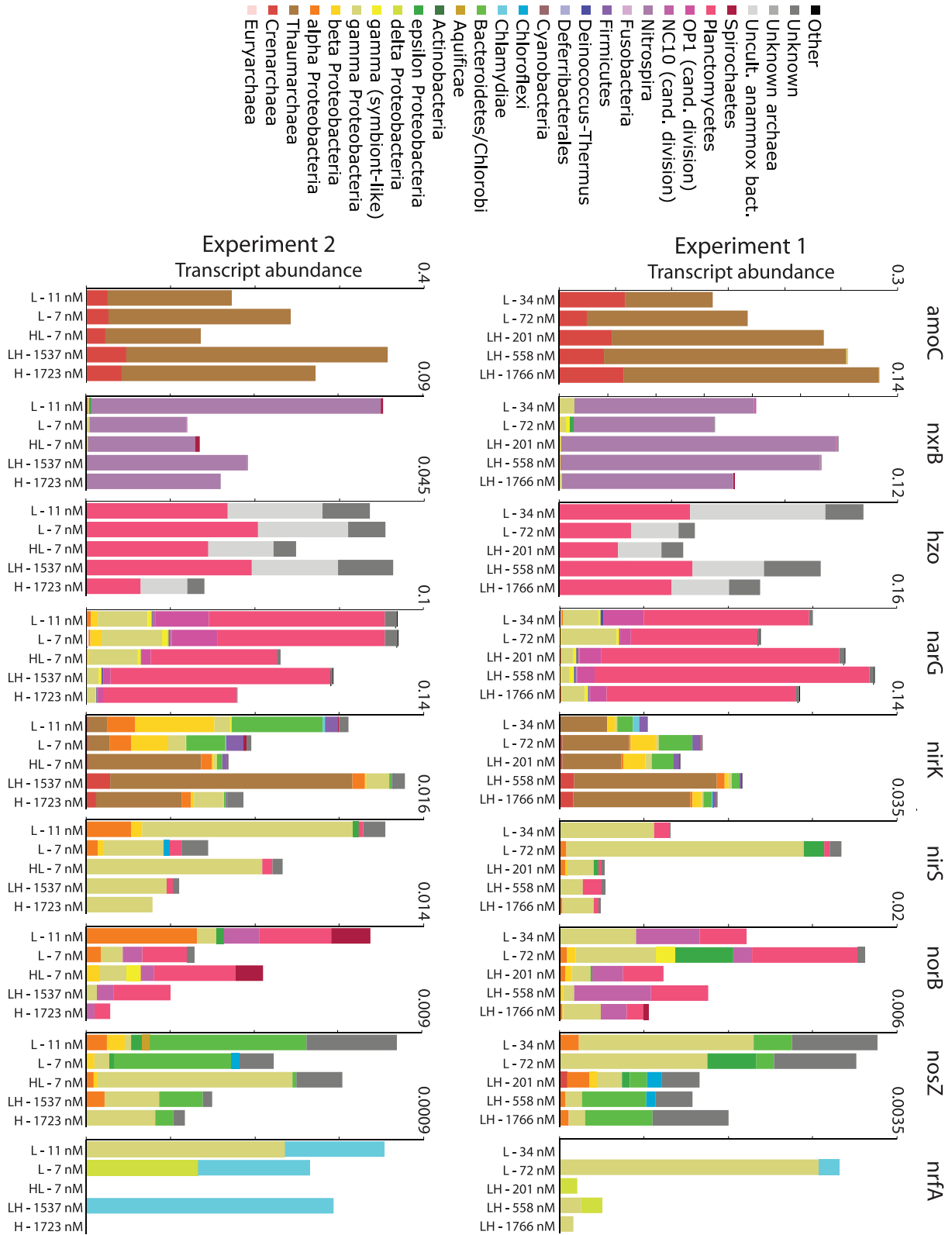


**FIG 6** Taxonomic representation and relative abundance of reads matching key nitrogen genes at different oxygen levels in bioreactor experiment 1 (right) and 2 (left). Transcript abundance is calculated as read count per gene per kilobase of gene length and then standardized as a percentage of total protein-coding reads per data set. Taxonomic identifications are based on annotations of NCBI reference sequences identified as top matches (above a bit score of 50) in BLASTX searches. Note that the y axis scales differ. Abbreviations for oxygen treatments are as in Fig. 5, and genes are as in Fig. 1.

tions reflective of *in situ* conditions in the OMZ off Chile. Inhibition of anammox and denitrification activity was observed over the O<sub>2</sub> concentration ranges applied in this study (5 to 2,000 nM), suggesting that the experimental O<sub>2</sub> conditions were ecologically relevant (Fig. 3). In contrast, patterns in transcript abundance at the endpoint of each experiment were not unambiguously linked to trends in the rate data. Nonetheless, some genes showed consistent patterns in response to O<sub>2</sub> amendment. Together, these data highlight the potential effects of O<sub>2</sub> fluctuation on dissimilatory nitrogen transformations in OMZ waters, as well as the extent to which community transcriptome patterns can complement and inform process rate measurements in experimental systems.

**Rates of anammox and denitrification and effects of O<sub>2</sub>.** We quantified bulk anammox and denitrification activity by measuring gas (N<sub>2</sub> and N<sub>2</sub>O) production and analyzed the expression of the genes coding for known enzymes catalyzing individual steps of these processes. In these experiments, <sup>15</sup>N<sub>2</sub> accumulated linearly immediately after the experiments were started, indicating that anammox and denitrification were active *in situ*. This was evidenced further by transcription of indicator genes for both anammox and denitrification (*hzo*, *nar*, *nir*, *nor*, and *noz*) in source water at the time of reactor filling, often at higher relative levels than those observed at the experiment endpoints (see the supplemental methods and Fig. S1 in the supplemental material). We suggest that the rates measured during the first part of the experiments, with linear increases in <sup>15</sup>N<sub>2</sub> concentrations, provide a measure of the *in situ* activity, under the assumption that the O<sub>2</sub> levels here did not inhibit the processes significantly (see below). Anammox and denitrification activity started as soon as the helium sparging stopped and O<sub>2</sub> had been removed (Fig. 2C), with linear increases in <sup>15</sup>N<sub>2</sub> concentrations over time. Addition of O<sub>2</sub> to a concentration of about 2 μM almost completely and rapidly inhibited these processes (Fig. 2B). These trends suggest an inhibition at the enzyme level, allowing immediate resumption of activity as soon as O<sub>2</sub> levels fall below inhibiting concentrations. If enzyme synthesis had been required for the resumption of anammox and denitrification activity, the transition to active N gas production would have been less abrupt and the rates would have increased over time. Indeed, the denitrifier *Paracoccus denitrificans* in pure culture at optimal temperature required 10 to 24 h to establish a fully active denitrification enzyme system after a shift from aerobic (90% air saturation) to anaerobic conditions (37, 38). Likewise, if inhibition had occurred at the enzyme production level (transcription or protein synthesis), the reduction in process rates presumably would have been much less abrupt, as residual proteins would have continued to function until internal enzyme levels became depleted. Thus, the response of both metabolic activity and gene expression to changes in O<sub>2</sub> concentration show that the organisms involved in nitrogen transformations are well adapted to an environment where O<sub>2</sub> concentrations fluctuate from anoxia to a few micromolar units on a time scale of hours to days, exactly as is the case around the oxic-anoxic interface where our samples were retrieved (e.g., see reference 39).

The rates of fixed-nitrogen removal (sum of anammox and denitrification) found here (in the first half of the control incubations) (Table 2) compare generally well with the rates measured previously at two stations approximately 10 km east and southeast of station 3 (40) and with the rates measured with the standard Exetainer method during the cruise (39). Also, the rates measured

by Dalsgaard et al. (14), at a station (G04) coinciding with our station 5, were in the same range as the rates found in the present study. Furthermore, the rates of anammox were within the range found off Peru by Kalvelage et al. (16) (see the work of Dalsgaard et al. [14] for a more thorough comparison of measured rates in the eastern South Pacific). While the fixed-nitrogen removal rates from the reactor experiments were in the same range as rates from previous cruises in the area, the high contribution of denitrification for N<sub>2</sub> production was found in only one previous survey (14). As suggested by Dalsgaard et al. (14), this may be controlled by the availability of electron donors for denitrification. However, O<sub>2</sub> contamination may also play a role. Exetainer incubations, which were used in most of the published OMZ denitrification/anammox studies, are most likely contaminated with a few hundred nM O<sub>2</sub> (31). If the higher sensitivity of denitrification than anammox to O<sub>2</sub> (see below) is a general phenomenon, denitrification may have been inhibited more than anammox in previous studies, potentially leading to an underestimate of the role of denitrification. The O<sub>2</sub> concentrations in the control reactors in the present study were probably lower than in most Exetainer incubations, which may have contributed to the observed higher contribution of denitrification to removal of fixed N.

The rates observed during the second half of the incubations were different from those observed during the first half, probably due to some sort of a bottle effect. In contrast to most of the published studies on anammox and denitrification in OMZs, we were able to identify and quantify this nonlinearity due to frequent sampling for N gas production. Furthermore, we were able to quantify O<sub>2</sub> contamination. While the rates obtained during the second part of the experiments do not represent *in situ* rates, the same suite of processes continued from the first half of the experiment. Thus, O<sub>2</sub> inhibition kinetics were investigated by comparing the rates from O<sub>2</sub>-amended reactors to the rates that were expected in the absence of O<sub>2</sub> manipulation (see equation 3 below). Another consequence of enclosing the water in a bottle was that in some of the experiments, N<sub>2</sub>O accumulated to concentrations higher than are normally found *in situ*. We have no explanation for this, but we assume that the same enzymes are active in the bioreactors and *in situ* and, as argued above, that the experimentally determined O<sub>2</sub> inhibition kinetics may be applied to *in situ* conditions.

The O<sub>2</sub>-dependent inhibition of N<sub>2</sub> production by anammox and of N<sub>2</sub> and N<sub>2</sub>O by denitrification was concentration dependent, with anammox showing a more variable response to O<sub>2</sub> amendments, while denitrification was more sensitive to O<sub>2</sub> (Fig. 3). Consequently, the C<sub>50</sub> for anammox (886 nM O<sub>2</sub>) is less well supported than that of denitrification (255 nM O<sub>2</sub> for total denitrification) (Table 3). While anammox was less sensitive to O<sub>2</sub> amendments than denitrification in the present study, the data also indicate that anammox was much more sensitive to O<sub>2</sub> than previously found. Indeed, 50% inhibition of anammox was achieved at 11 to 16 μM in the OMZ off Namibia and from 2 to 11 μM off Peru (22), which is in line with results from the Black Sea, where anammox was reduced by 7 to 8% at about 1 μM O<sub>2</sub> and was fully inhibited by 13 μM O<sub>2</sub> (21). Kalvelage et al. (22) observed a tendency for anammox to become more sensitive to O<sub>2</sub> at stations seaward of the continental shelf, where one station showed no anammox above 2.8 μM O<sub>2</sub>. A very similar result was obtained by Babbin et al. (23) from the eastern tropical North Pacific, where anammox still occurred at low rates at 3 μM O<sub>2</sub> and



was completely inhibited at 8  $\mu\text{M}$   $\text{O}_2$ . The two latter observations are very much in line with our results from the two off-shelf stations off Iquique, Chile, where anammox was recorded at up to 1.7  $\mu\text{M}$   $\text{O}_2$  in two of the experiments (Fig. 3). The fact that the  $\text{O}_2$  threshold observed in the present study is substantially lower than that found in most previous studies may partly be explained by variation in microbial community composition among studies. It is also possible that activity observed at higher  $\text{O}_2$  bulk levels in previous studies in fact occurred in  $\text{O}_2$ -depleted microzones within aggregates (22, 39). Furthermore, these studies all used nonstirred Exetainer incubations. Organisms and particulates may settle out of suspension during such incubations, creating a local low- $\text{O}_2$  environment at the bottom of the vials, where anaerobic processes may be active at what appear to be relatively high  $\text{O}_2$  concentrations. This would not happen in the stirred bioreactors in the present study, and furthermore, the stirring would increase  $\text{O}_2$  transport into aggregates, leading to a smaller difference between  $\text{O}_2$  concentrations inside and outside aggregates. Consequently, stirred incubations may produce  $\text{O}_2$  sensitivity results that more accurately reflect the responses of the individual organisms.

The  $\text{O}_2$  sensitivities of  $\text{N}_2\text{O}$  and  $\text{N}_2$  production by denitrification were similar, requiring 200 and 300 nM  $\text{O}_2$  for 50% inhibition, respectively (Table 3). As most studies of nitrogen removal in OMZs have failed to detect canonical denitrification, experimental evidence of the effect of  $\text{O}_2$  on this process is scarce. However, in one recent  $^{15}\text{N}$ -labeling study, denitrification was measurable and  $\text{O}_2$  amendment experiments showed that at 3  $\mu\text{M}$   $\text{O}_2$ , denitrification was completely inhibited (23). This level is certainly higher than the threshold found in the present study, but since concentrations between 3  $\mu\text{M}$  and anoxia were not tested by Babbitt et al. (23), these studies do not contradict each other. In the present study, effects of  $\text{O}_2$  on process rates generally agree well with the metatranscriptomic data. In the experimental reactors with  $\text{O}_2$  levels from ~200 to 1,800 nM, *nosZ* transcript abundances were consistently lower than in the controls, which had  $\text{O}_2$  levels in the tens of nanomolar units. Similarly, inhibition of the transcription of *nirS*, *nrfA*, and *norB* denitrification genes already occurred at the lowest  $\text{O}_2$  amendment (201 nM), agreeing with the suggested halt of  $\text{N}_2$  production in the eastern South Pacific OMZ when  $\text{O}_2$  is detectable *in situ* (14) and with studies of cultured denitrifiers showing *nirS* and *norB* transcription sensitivity at an  $\text{O}_2$  concentration of <~0.5  $\mu\text{M}$  (41–44).

In contrast, the transcription of *nirK*-like nitrite reductase, which was predominantly affiliated with archaea and hence likely with ammonium oxidizers, appeared not to be largely affected by  $\text{O}_2$  exposure, consistent with the results obtained with a *nirK*-utilizing denitrifier (43). The fact that the  $\text{N}_2\text{O}$ -producing and -consuming parts of denitrification otherwise react similarly to  $\text{O}_2$  exposure suggest that low-range fluctuations in  $\text{O}_2$  concentrations will not cause substantial  $\text{N}_2\text{O}$  accumulation from denitrification. The production of  $\text{N}_2\text{O}$  by ammonium oxidizers may respond differently, however.

We did not quantify the  $\text{O}_2$  sensitivity of  $\text{NO}_3^-$  reduction activity in this study. However, the transcriptome data generated here show no clear suppression of bulk nitrate reductase gene (*narG*) transcription within the range of  $\text{O}_2$  concentrations applied (<2  $\mu\text{M}$ ) (Fig. 5). At a first glance, this suggests that  $\text{NO}_3^-$  reduction was less sensitive to  $\text{O}_2$  than the other steps in the denitrification pathway. However, the majority of the *narG* transcripts

were affiliated with *narG* of anammox bacteria (“*Ca. Scalindua*” and “*Ca. Kuenenia*”), which likely use this enzyme oxidatively to drive reverse electron transport (35, 45). Closer inspection of the *narG* transcript pool suggests that  $\text{NO}_3^-$  reduction gene expression may in fact be inhibited in some taxonomic groups, notably the *Gammaproteobacteria*, by  $\text{O}_2$  concentrations as low as 200 nM (Fig. 6). This result is in contrast to results for some organisms that exhibit relatively stable nitrate reductase expression. In the human pathogen *Mycobacterium tuberculosis*, for example, a NarGH nitrate reductase is constitutively expressed, with enzyme levels independent of oxygen concentrations (46). Nitrate reduction to nitrite in this bacterium is instead regulated via a nitrate transporter (NarK), whose transcription and activity are inhibited not directly by the presence of molecular oxygen but by the redox state of the cell, allowing a rapid switch to nitrate utilization when transitioning from oxidizing to reducing conditions (47). In contrast, studies of complex multispecies communities in OMZs have described variable and relatively weak effects of  $\text{O}_2$  on nitrate reduction rates. For example, no effect of  $\text{O}_2$  at concentrations of up to 25  $\mu\text{M}$  was found at one station in the Peruvian OMZ, but reductions in nitrate reduction rates of up to 50% when  $\text{O}_2$  reached 4  $\mu\text{M}$  at other stations off Peru and in the Namibian OMZ were reported (22). This variability in the sensitivity of nitrate reduction to  $\text{O}_2$  may be due partly to differences among microbial communities at the sampling sites but also to variations in other chemical parameters, potentially including nitrate or nitric oxide, which have been shown to regulate nitrate reductase transcription or activity (47, 48).

The relative abundances of denitrification and anammox gene transcripts highlight the potential for decoupling between transcriptional patterns (at the end of the experiment) and the observed biochemical response to  $\text{O}_2$ . Notably, endpoint anammox-associated gene transcripts (e.g., *hzo* and “*Ca. Scalindua*”-like *nirS*) did not vary appreciably or consistently in relative abundance between the low- $\text{O}_2$  control and  $\text{O}_2$  addition treatments (Fig. 5), whereas  $\text{O}_2$  addition clearly inhibited anammox activity (Fig. 3). It is possible that variations in anammox gene transcription occurred between control and amendment reactors earlier in the experiments and that due to the short half-life of mRNA (minutes or hours), such differences were not captured by endpoint sampling. However, assuming that transcript abundances were equivalent among treatments at the start of experiments, it is hard to envision variations in transcription that explain both the observed enzyme inhibition and the endpoint transcript patterns. The potential alternative would be that  $\text{O}_2$  at low levels does not inhibit transcription to the same extent as it inhibits protein function, i.e., that regulation occurs at the posttranscriptional level for anammox enzymes, within the range of conditions tested here. Other genes involved in dissimilatory nitrogen metabolism, notably the denitrification genes *nirS*, *norB*, and *nosZ* (as well as genes involved in aerobic  $\text{NH}_4^+$  oxidation [*amoC*]; see the supplemental material), showed a tighter coupling to  $\text{O}_2$  levels. These results reinforce prior studies showing that distinct steps of multistep metabolic pathways, such as denitrification, can differ in  $\text{O}_2$  sensitivity (43). Consequently, discrepancies in estimates of the sensitivity of bulk denitrification and anammox to  $\text{O}_2$  (discussed above) are likely due to a combination of taxonomic variation as well as differences in sensitivity among the various enzymes of each pathway. This is particularly likely for denitrification, in which the overall pathway is mediated by diverse assemblages of

bacteria (49–51). Taxonomic analysis of gene transcripts suggested that there is high taxonomic diversity among the denitrifiers and that the taxonomic composition of the individual denitrification gene assemblies was highly variable, indicating that the denitrification process is indeed the result of a series of individual reactions catalyzed by different groups of organisms. Together, these data indicate that the extent to which transcript abundance patterns in metatranscriptional data sets can be used as proxies for process rate measurements is variable, likely due to complex factors, including the relative dominance of different community members, differences in the level of metabolic regulation (transcriptional, translational, and enzymatic), and the range of environmental conditions being observed.

**Effects of sulfide.** Genomic analysis has indicated a significant role of sulfur cycling in the OMZs (28, 52, 53) contributing to the discovery of a cryptic sulfur cycle (10). This cycle involves the reduction of sulfate to sulfide, which is immediately oxidized and accumulates only under special circumstances in the absence of  $\text{NO}_3^-$  and  $\text{NO}_2^-$  in OMZs without sediment contact (54). Under normal OMZ conditions with high concentrations of  $\text{NO}_3^-$  and  $\text{NO}_2^-$ ,  $\text{NO}_3^-$  reduction or denitrification is responsible for removal of  $\text{H}_2\text{S}$ . In a situation with  $\text{H}_2\text{S}$  accumulation, mainly resulting from  $\text{H}_2\text{S}$  release from the sediment,  $\text{H}_2\text{S}$  was shown to be the major electron donor and  $\text{NO}_3^-$  or  $\text{NO}_2^-$  to be the terminal electron acceptor through all the individual steps of the denitrification process (55, 56). It is not clear to what degree  $\text{H}_2\text{S}$  was the direct electron donor for  $\text{NO}_3^-$  reduction or denitrification in these experiments. However, in the  $\text{H}_2\text{S}$ -amended reactors, denitrification to  $\text{N}_2\text{O}$  was strongly stimulated in the second half of the experiment (Fig. 4), supposedly as a result of  $\text{H}_2\text{S}$  being a quantitatively important electron donor. The effect of  $\text{O}_2$  on denitrification in the presence of  $\text{H}_2\text{S}$  was very similar to the effects seen without added  $\text{H}_2\text{S}$  (Fig. 2). This might suggest that the same organisms were active in both experiments or, alternatively, that different groups were active but had similar sensitivities to  $\text{O}_2$ . The latter is supported by the delayed response of denitrification to sulfide amendment, which indicates an induction period for the sulfide-oxidizing community. Sulfide amendment may also have stimulated  $\text{NO}_3^-$  reduction to  $\text{NO}_2^-$  as previously observed (10), but the precision of our  $\text{NO}_2^-$  measurements was not sufficient to quantify this process. It has previously been suggested that  $\text{H}_2\text{S}$  may interfere with the nitrogen cycle by inhibiting anammox (27, 55), and complete inhibition of the process at concentrations of 1.5 to 2.5  $\mu\text{M}$  was observed in Black Sea waters (21). In contrast, we found no significant inhibitory effect of ca. 1  $\mu\text{M}$   $\text{H}_2\text{S}$  on anammox (Fig. 4). Also, the reduction of  $\text{N}_2\text{O}$  in the denitrification pathway may be inhibited by  $\text{H}_2\text{S}$  (57), but such inhibition was relatively minor in our experiments. During the first half of the experiment,  $\text{N}_2\text{O}$  accounted for 74% and 92% of total gas production in the absence and presence of  $\text{H}_2\text{S}$ , respectively. These values were 77% and 94% during the second half. This low degree of inhibition is probably due to the low  $\text{H}_2\text{S}$  concentrations in the experiment (ca. 1  $\mu\text{M}$ ). In the anoxic water column of the Baltic Sea, the ratio of  $\text{N}_2\text{O}$  to total gas production was proportional to the  $\text{H}_2\text{S}$  concentration, and first at a concentration of 7  $\mu\text{M}$   $\text{H}_2\text{S}$ ,  $\text{N}_2\text{O}$  accounted for half of the total gas production from denitrification (58). In pelagic OMZs,  $\text{H}_2\text{S}$  only rarely accumulates to the levels applied in our experiments (55). However, in OMZs with sediment contact and in a global warming scenario with expand-

ing OMZs (4), sulfide accumulation may occur more frequently (6, 55, 56), potentially leading to  $\text{N}_2\text{O}$  production.

## MATERIALS AND METHODS

**Study area.** Sampling took place in the eastern South Pacific OMZ off Iquique in northern Chile during the Microbial Oceanography of Oxygen Minimum Zones (MOOMZ-III) cruise on the R/V *Agor Vidal Gormaz* from 8 to 18 January 2010. At this site,  $\text{O}_2$ -deficient equatorial subsurface water is transported southward by the Peru-Chile undercurrent, and the  $\text{O}_2$ -rich surface water is transported north by the Humboldt current (40). Water was sampled at two locations 30 km (station 3; 20°06'S, 70°25'W) and 69 km (station 5; 20°06'S, 70°48'W) offshore (10). At station 3, water was collected at depths of 75 m (specific density [ $\sigma_\theta$ ], 26.23  $\text{kg m}^{-3}$ ) and 82 m ( $\sigma_\theta$ , 26.22  $\text{kg m}^{-3}$ ) for experiments 1 and 3, respectively, and at station 5, water was collected at 86 m ( $\sigma_\theta$ , 26.21  $\text{kg m}^{-3}$ ) for experiment 2. The oxic-anoxic (anoxic =  $\text{O}_2$  below the detection limit of the STOX sensor; see below) interface was at 70- and 75-m depths at station 3 during sampling for experiments 1 and 3, respectively, and at 80 m at station 5 during sampling for experiment 2.

**Reactors.** The reactors used for incubations were described previously (32). Briefly, reactors were 2-liter glass cylinders with a PVC piston with two O rings fitting tightly inside the glass cylinder. The end of the piston was covered with a glass plate to prevent leakage of  $\text{O}_2$  into the incubating water. The glass plate was penetrated with three pieces of PEEK (Upchurch Scientific) tubing to allow gassing, amendment, and sampling. A highly sensitive switchable trace oxygen (STOX) sensor (17, 18) was placed in each of the eight parallel reactors. Water was sampled using a pump profiling system (PPS) (10), which allowed pumping of water from the  $\text{O}_2$ -depleted zone directly into the reactors. The pump system was equipped with a Seabird 25 CTD and both a standard SBE 43  $\text{O}_2$  sensor and a STOX sensor, and  $\text{O}_2$  concentrations were monitored continuously during sampling. Filling of the reactors was described in detail earlier (32). Briefly, the reactor was flushed with nitrogen and then filled with water from below with a counterflow of nitrogen. The water was allowed to overflow for three volume changes before the reactor was sealed. The reactors were transferred to the onboard lab, placed in water at the *in situ* temperature (ca. 13°C), and protected from light. Circulation inside the reactor was created by a glass-coated, 2-cm-long magnetic stir bar rotating at ca. 60 rpm. Standard Teflon-coated stir bars contain large amounts of  $\text{O}_2$ , which would be released to the incubating water and raise the  $\text{O}_2$  concentration in the experiments.

**Incubation experiments.** Three incubation experiments (28 to 36 h each) were conducted to examine the effects of  $\text{O}_2$  concentration on denitrification and anammox rates and community gene expression. Each experiment involved 7 to 8 reactors representing a range of  $\text{O}_2$  concentrations from ~10 to 50 nM to 2  $\mu\text{M}$  (Table 1). Each reactor was equipped with a STOX sensor and purged with a gentle flow of helium through 1/16-in. PEEK tubing for ca. 1.5 h, which removed the  $\text{O}_2$  that had entered during handling, typically 30 to 60 nM with some variation (Table 1). During purging, some  $\text{CO}_2$  was removed, causing the pH to increase by ~0.3. Subsequently, all headspace and bubbles were removed, and water samples were taken to measure initial concentrations of  $\text{NO}_3^-$ ,  $\text{NO}_2^-$ , and  $\text{NH}_4^+$ . All reactors were then amended with  $^{15}\text{NO}_2^-$  to a target concentration of 10  $\mu\text{M}$ . *In situ*  $\text{NO}_2^-$  concentrations were in the range of 2.2 to 6.7  $\mu\text{M}$ , and  $^{15}\text{NO}_2^-$  constituted 59 to 86% of the total  $\text{NO}_2^-$  pool, as determined from concentrations before and after amendment.

All three experiments involved the manipulation of reactor  $\text{O}_2$  concentrations. Each experiment included two control reactors that were filled, gassed, incubated, and sampled in parallel to the manipulated reactors. In these controls, the  $\text{O}_2$  concentrations were kept as low as possible (designated “L” in Table 1; for an example, see Fig. 2A) in order to represent *in situ* conditions. In some reactors,  $\text{O}_2$  was kept low through the first half of the experiment and then raised to a target concentration of 200 nM, 500 nM, or 2  $\mu\text{M}$  (low to high, designated “LH” in Table 1; for an example, see Fig. 2B), while others followed the opposite scheme, with high  $\text{O}_2$  from

the start of the experiment lowered to the low nM range halfway through (high to low, designated “HL” in Table 1; for an example, see Fig. 2C). Finally, in some reactors, O<sub>2</sub> was kept high throughout the experiment (designated “H” in Table 1). Oxygen was added by injecting air-saturated water obtained from the station when the reactors were filled (1 ml injected gave a rise of ca. 170 nM O<sub>2</sub>). Oxygen was removed by purging with helium as described above. In the experiments where O<sub>2</sub> concentrations were raised, air-saturated water was injected at a sufficient frequency to counteract O<sub>2</sub> consumption and maintain the target O<sub>2</sub> concentration range. In the experiments starting with high O<sub>2</sub> concentrations, air-saturated water was injected right after the initial gassing with helium. The increase in O<sub>2</sub> concentration after injection of air-saturated seawater was instantaneous, whereas removal of O<sub>2</sub> by helium sparging took about 1 h. In experiment 3, a solution of NaS<sub>2</sub> (5 mM) was added to some of the reactors to a concentration of ca. 1 μM. There was no systematic change in total sulfide concentration in experiment 3 after sulfide was added, and the actual concentrations are given as the average throughout the experiment (Table 1). The times from sampling until start of the experiment (i.e., tracer amendment) were 10, 9, and 5 h in experiments 1, 2, and 3, respectively.

Samples for N<sub>2</sub> and N<sub>2</sub>O gas isotopic composition and concentration and for NO<sub>2</sub><sup>-</sup>, NO<sub>3</sub><sup>-</sup>, and NH<sub>4</sub><sup>+</sup> concentrations were taken eight times at approximately regular intervals during the 28- to 36-h-long incubations. Samples for nitrogen gas were stored in 12-ml glass vials with a butyl rubber septum (Exetainer; Labco) preserved with 100 μl 50% (wt/vol) ZnCl<sub>2</sub>. Samples for NO<sub>2</sub><sup>-</sup> (experiments 1 and 2) and NH<sub>4</sub><sup>+</sup> were analyzed immediately, whereas samples for NO<sub>2</sub><sup>-</sup> in the presence of sulfide (experiment 3) and all NO<sub>3</sub><sup>-</sup> samples were frozen for later analysis. Endpoint samples for gene expression analysis were obtained by filtering the remaining water in each reactor.

**Chemical analysis.** Concentrations of NO<sub>3</sub><sup>-</sup> plus NO<sub>2</sub><sup>-</sup> were measured as NO after reduction in hot vanadium chloride (59) on a Thermo Environmental Instruments 42c NO<sub>x</sub> analyzer. Nitrite in the absence of sulfide was measured using a standard colorimetric technique (60), and NO<sub>2</sub><sup>-</sup> in the presence of sulfide was analyzed as NO after reduction in cold vanadium chloride (59). Ammonium was quantified fluorometrically by the orthophthaldialdehyde method (61) on a Turner Designs Trilogy fluorometer, and sulfide concentration was quantified colorimetrically according to the method of Cline (62). Nitrogen isotopes in N<sub>2</sub> and N<sub>2</sub>O were analyzed on a Thermo Delta V Plus isotope ratio mass spectrometer as described previously (14).

**Calculations.** Rates of anammox and denitrification in the <sup>15</sup>NO<sub>2</sub><sup>-</sup> amended experiments were calculated as described earlier (63). Briefly, knowing the mole fraction of <sup>15</sup>N in the NO<sub>2</sub><sup>-</sup> pool ( $F_N$ ) and the production rates of <sup>29</sup>N<sub>2</sub> ( $P_{29}$ ) and <sup>30</sup>N<sub>2</sub> ( $P_{30}$ ), N<sub>2</sub> production by anammox and denitrification were calculated as follows:

$$\text{denitrification} = P_{30} \times F_N^{-2} \quad (1)$$

$$\text{anammox} = F_N^{-1} \times [P_{29} + 2 \times (1 - F_N^{-1}) \times P_{30}] \quad (2)$$

$F_N$  was estimated from the concentrations of NO<sub>2</sub><sup>-</sup> before and after amendment of <sup>15</sup>NO<sub>2</sub><sup>-</sup>, and  $P_{29}$  and  $P_{30}$  were calculated as the slopes of the linear regression of <sup>29</sup>N<sub>2</sub> and <sup>30</sup>N<sub>2</sub> concentrations as a function of time. Production of N<sub>2</sub>O by denitrification was estimated using equation 1 replacing  $P_{30}$  with the production rate of <sup>46</sup>N<sub>2</sub>O, which was calculated as the slope of the linear regression of <sup>46</sup>N<sub>2</sub>O versus time. Manipulation of O<sub>2</sub> concentrations took place immediately after the fourth sampling in all experiments, and rates of anammox and denitrification were calculated in each incubation for the period from the first to the fourth sampling (referred to as the first half) (Table 1) and from the fourth to the eighth sampling (referred to as the second half) (Table 1). Dissimilatory nitrite reduction to ammonium (DNRA) was not detectable in parallel incubations from the two stations (39), and hence we ruled out the possibility that denitrification could be substantially overestimated due to a coupling of DNRA and anammox. This is consistent with the very low expression of the *nrfA* gene (see Results), coding for a key enzyme in the DNRA path-

way. Furthermore, the N<sub>2</sub>O production recorded during incubations and the expression of the genes coding for denitrification enzymes (see results) indicate that denitrification was indeed active.

The effects of O<sub>2</sub> concentration on rates of anammox and denitrification were evaluated by comparing rates from the first half to rates from the second half of the incubation in the manipulated reactors. However, process rates also changed from the first to the second half in the control reactors with continuously low O<sub>2</sub> concentrations. It was assumed that rates in the manipulated reactors would have undergone the same relative change from the first half to the second half of the incubation if they had not been manipulated. Therefore, the effect of the change in O<sub>2</sub> concentration was estimated by comparing the measured rate during the second half of the incubation with the rate expected in the absence of manipulation. There was one set of control reactors for each of the three experiments, and manipulated reactors of one experiment were compared to control reactors from that same experiment. The expected rate in the absence of manipulation ( $R2_{\text{expected}}$ ) was calculated as

$$R2_{\text{expected}} = R1 \times (Rc2/Rc1) \quad (3)$$

where  $R1$  is the rate measured during the first half of the incubation and  $Rc1$  and  $Rc2$  are the rates measured in the control during the first and second halves of the incubation. The inhibition of the rate due to a change in O<sub>2</sub> concentration halfway through the incubation was calculated as

$$\text{Inhibition} = -(R2 - R2_{\text{expected}})/R2_{\text{expected}} \times 100 \quad (4)$$

where  $R2$  is the rate measured during the second half of the incubation. The calculated inhibition was plotted individually for each process (N<sub>2</sub>, N<sub>2</sub>O, and N<sub>2</sub> + N<sub>2</sub>O production by denitrification and N<sub>2</sub> production by anammox) as a function of the average O<sub>2</sub> concentration during the second half of the incubation, and data were fitted to the exponential function

$$\text{inhibition}(\%) = 1 - e^{-k \times C} \quad (5)$$

using the Levenberg-Marquardt algorithm (Origin 9.0; OriginLab, MA), where  $C$  is the O<sub>2</sub> concentration and  $k$  is the variable coefficient (modified from the work of Jensen et al. [64], where rates, rather than relative inhibition, were fitted as a function of inhibitor concentration). From this, the O<sub>2</sub> concentration resulting in a 50% inhibition of the rates,  $C_{50}$ , was calculated.

**Analysis of gene expression.** Although enclosure in bioreactors has been shown to alter the metatranscriptional profile of some OMZ community members (i.e., bottle effects) (32), comparisons between bioreactors with contrasting oxygen treatments can help identify gene expression patterns suggestive of differential oxygen sensitivity. High sequencing costs and problems with sample loss during processing prevented replicate sequencing for all treatments, excluding the four low-oxygen controls (Table 1). Therefore, samples for community gene expression analysis were collected from a subset of bioreactors (Table 1). Sample processing and analysis were as described previously (32). Briefly, the endpoint microbial community was collected by filtering the water remaining in each bioreactor (~1.2 liters) at the endpoint of the experiment. Water was filtered through a glass fiber prefilter (47 mm, 1.6 μm GF/A; Whatman) and then a primary collection filter (0.22 μm; Sterivex) using a peristaltic pump. Sterivex cartridges were filled with RNAlater (Ambion), capped, flash-frozen in liquid nitrogen, and stored at -80°C. Less than 15 min elapsed between sample collection (experiment end) and flash-freezing.

Community RNA was extracted using a modification of the mirVana microRNA (miRNA) isolation kit (Ambion) as described by Stewart et al. (32). Briefly, filters were thawed on ice, and the RNAlater surrounding each filter was expelled via syringe and discarded. Cells were lysed directly on the filter by adding lysis/binding and miRNA homogenate additive (Ambion) and vortexing. Lysate was expelled, and nucleic acids were isolated by treatment with acid-phenol-chloroform according to the manufacturer's protocol. Extracted total RNA was treated with DNase (Turbo DNA free) to eliminate genomic DNA and purified using the RNeasy MinElute cleanup kit (Qiagen).

Prokaryotic and eukaryotic rRNA was removed from RNA extracts via a subtractive hybridization protocol (65) using sample-specific probes developed by Stewart et al. (32). rRNA-depleted RNA was linearly amplified, converted to double-stranded cDNA, and purified as described previously (28, 32, 66). Purified cDNA was sequenced on a Roche FLX genome sequencer using Titanium series chemistry (one full plate per sample, excluding the control [low-O<sub>2</sub>] bioreactor replicates, which were sequenced using a half-plate run each). Metatranscriptome data sets describing gene expression patterns in the control bioreactors ( $n = 4$ ) (Table 1) and from the *in situ* microbial community (filtered from source water at the time of bioreactor filling;  $n = 2$ ) (Fig. 6) were published previously (32) and are available in the NCBI Sequence Read Archive under accession number SRA049608.1. The data for 6 bioreactors amended with O<sub>2</sub> in experiments 1 and 2 (Table 1) are published here. Sequencing reads counts for these data sets are in Table S1.

Metatranscriptomes were analyzed as described previously (28, 32). Duplicate reads (100% similarity, identical lengths), potentially arising from pyrosequencing errors, were identified using CD-HIT (67) and removed from each data set. rRNA transcripts were identified by BLASTN (bit score threshold = 50) against a database of prokaryotic and eukaryotic rRNA sequences compiled from the ARB-SILVA databases and excluded from further analysis. Protein-coding mRNA transcripts were identified by BLASTX against the NCBI nonredundant (nr) protein database (as of April 2012), modified to include the published genome of the marine anammox bacterium "*Candidatus Scalindua profunda*" (36) (data from Joint Genome Institute, U.S. Department of Energy). For reads matching multiple reference genes with equal bit scores, each reference was counted as a top match, with its count scaled in proportion to the number of genes sharing the top score.

The relative abundances of key N cycle genes (Fig. 5 and 6) were determined via keyword searches of BLASTX results (bit score > 50), as described by Canfield et al. (10) and Ganesh et al. (68). NCBI nr genes representing top BLASTX matches were recovered from GenBank, and each database entry was examined manually to confirm gene identity. Entries with ambiguous annotations were further verified by BLASTX. Gene abundances were normalized based on best approximate gene length (bp), estimated from full-length open reading frames from sequenced genomes: *amoC* (750 bp), *nxrB* (1,500 bp), *hzo* (1,650 bp), *narG* (3,600 bp), *nirK* (1,140 bp), *nirS* (1,620 bp), *nrfA* (1,440 bp), *norB* (1,410 bp), and *nosZ* (1,950 bp). Sequence counts per kilobase of target gene were normalized to data set size (Fig. 6) and to counts of sequences matching the universal, single-copy gene encoding RNA polymerase subunit B (*rpoB*, 4,020 bp) (Fig. 5) as described by Ganesh et al. (68), such that a value of 1 in Fig. 5 indicates abundance equivalent to that of *rpoB* (assuming the gene lengths listed above). The taxonomic identities of transcripts were inferred from the matching reference gene annotations, with relative taxon abundances tabulated using MEGAN 4 (69) and shown by color coding in Fig. 6.

**Data accession number.** All sequence data generated in this paper can be accessed at NCBI under BioProject ID [PRJNA263804](http://www.ncbi.nlm.nih.gov/BioProject/PRJNA263804).

## SUPPLEMENTAL MATERIAL

Supplemental material for this article may be found at <http://mbio.asm.org/lookup/suppl/doi:10.1128/mBio.01966-14/-/DCSupplemental>.

Text S1, PDF file, 0.1 MB.

Figure S1, PDF file, 0.1 MB.

Table S1, PDF file, 0.04 MB.

## ACKNOWLEDGMENTS

We thank the captain and crew of the *Agor Vidal Gormaz* from the Chilean Navy for their kind support, Preben G. Sørensen for excellent assistance with the experiments, and Gadiel Alarcón for sampling and technical assistance.

This work was supported by the Agouron Institute and the Gordon and Betty Moore Foundation. T.D. was supported by the European Research Council Advanced Grant program through the OXYGEN project

(no. 267233-ERC) and the Arctic Research Centre (ARC), Aarhus University. We also thank the Danish National Research Foundation (Danmarks Grundforskningsfond grant DNRF53).

We declare no conflicts of interest.

This work is a contribution to the Arctic Science Partnership (ASP) (<http://asp-net.org>).

## REFERENCES

- Falkowski PG, Fenchel T, Delong EF. 2008. The microbial engines that drive Earth's biogeochemical cycles. *Science* 320:1034–1039. <http://dx.doi.org/10.1126/science.1153213>.
- Thamdrup B, Dalsgaard T, Revsbech NP. 2012. Widespread functional anoxia in the oxygen minimum zone of the eastern South Pacific. *Deep Sea Res. I* 65:36–45. <http://dx.doi.org/10.1016/j.dsr.2012.03.001>.
- Karstensen J, Stramma L, Visbeck M. 2008. Oxygen minimum zones in the eastern tropical Atlantic and Pacific oceans. *Prog. Oceanogr.* 77: 331–350. <http://dx.doi.org/10.1016/j.pocean.2007.05.009>.
- Diaz RJ, Rosenberg R. 2008. Spreading dead zones and consequences for marine ecosystems. *Science* 321:926–929. <http://dx.doi.org/10.1126/science.1156401>.
- Schmidt J. 1925. On the contents of oxygen in the ocean on both sides of Panama. *Science* 61:592–593. <http://dx.doi.org/10.1126/science.61.1588.592>.
- Ulloa O, Canfield DE, DeLong EF, Letelier RM, Stewart FJ. 2012. Microbial oceanography of anoxic oxygen minimum zones. *Proc. Natl. Acad. Sci. U. S. A.* 109:15996–16003. <http://dx.doi.org/10.1073/pnas.1205009110>.
- Revsbech NP, Jørgensen BB, Blackburn TH. 1980. Oxygen in the seabottom measured with a microelectrode. *Science* 207:1355–1356. <http://dx.doi.org/10.1126/science.207.4437.1355>.
- Froelich PN, Klinkhammer GP, Bender ML, Luedtke GR, Heath GR, Cullen D, Dauphin P. 1979. Early oxidation of organic matter in pelagic sediments of the eastern equatorial Atlantic: suboxic diagenesis. *Geochim. Cosmochim. Acta* 43:1075–1090. [http://dx.doi.org/10.1016/0016-7037\(79\)90095-4](http://dx.doi.org/10.1016/0016-7037(79)90095-4).
- Lam P, Kuypers MM. 2011. Microbial nitrogen cycling processes in oxygen minimum zones. *Ann. Rev. Mar. Sci.* 3:317–345. <http://dx.doi.org/10.1146/annurev-marine-120709-142814>.
- Canfield DE, Stewart FJ, Thamdrup B, De Brabandere L, Dalsgaard T, DeLong EF, Revsbech NP, Ulloa O. 2010. A cryptic sulfur cycle in oxygen-minimum-zone waters off the Chilean coast. *Science* 330: 1375–1378. <http://dx.doi.org/10.1126/science.1196889>.
- Gruber N, Sarmiento JL. 1997. Global patterns of marine nitrogen fixation and denitrification. *Glob. Biogeochem. Cycles* 11:235–266. <http://dx.doi.org/10.1029/97GB00077>.
- Codispoti LA, Brandes JA, Christensen JP, Devol AH, Naqvi SWA, Paerl HW, Yoshinari T. 2001. The oceanic fixed nitrogen and nitrous oxide budgets: moving targets as we enter the Anthropocene? *Sci. Mar.* 65(Suppl 2):85–105.
- Ward BB, Devol AH, Rich JJ, Chang BX, Bulow SE, Naik H, Pratihary A, Jayakumar A. 2009. Denitrification as the dominant nitrogen loss process in the Arabian Sea. *Nature* 461:78–81. <http://dx.doi.org/10.1038/nature08276>.
- Dalsgaard T, Thamdrup B, Fariás L, Revsbech PN. 2012. Anammox and denitrification in the oxygen minimum zone of the eastern South Pacific. *Limnol. Oceanogr.* 57:1331–1346. <http://dx.doi.org/10.4319/lo.2012.57.5.1331>.
- Lam P, Lavik G, Jensen MM, van de Vossenberg J, Schmid M, Woebken D, Gutiérrez D, Amann R, Jetten MS, Kuypers MM. 2009. Revising the nitrogen cycle in the Peruvian oxygen minimum zone. *Proc. Natl. Acad. Sci. U. S. A.* 106:4752–4757. <http://dx.doi.org/10.1073/pnas.0812444106>.
- Kalvelage T, Lavik G, Lam P, Contreras S, Arteaga L, Osler CR, Oschlies A, Paulmier A, Stramma L, Kuypers MMM. 2013. Nitrogen cycling driven by organic matter export in the South Pacific oxygen minimum zone. *Nat. Geosci.* 6:228–234. <http://dx.doi.org/10.1038/ngeo1739>.
- Revsbech NP, Larsen LH, Gundersen J, Dalsgaard T, Ulloa O, Thamdrup B. 2009. Determination of ultra-low oxygen concentrations in oxygen minimum zones by the STOX sensor. *Limnol. Oceanogr. Methods* 7:371–381. <http://dx.doi.org/10.4319/lom.2009.7.371>.
- Revsbech NP, Thamdrup B, Dalsgaard T, Canfield DE. 2011. Construction of STOX oxygen sensors and their application for determination of

- O<sub>2</sub> concentrations in oxygen minimum zones. *Methods Enzymol.* 486: 325–341. <http://dx.doi.org/10.1016/B978-0-12-381294-0.00014-6>.
19. Whitmire AL, Letelier RM, Villagrán V, Ulloa O. 2009. Autonomous observations of *in vivo* fluorescence and particle backscattering in an oceanic oxygen minimum zone. *Opt. Express* 17:21992–22004. <http://dx.doi.org/10.1364/OE.17.021992>.
  20. Lam P, Jensen MM, Lavik G, McGinnis DF, Müller B, Schubert CJ, Amann R, Thamdrup B, Kuypers MM. 2007. Linking crenarchaeal and bacterial nitrification to anammox in the Black Sea. *Proc. Natl. Acad. Sci. U. S. A.* 104:7104–7109. <http://dx.doi.org/10.1073/pnas.0611081104>.
  21. Jensen MM, Kuypers MM, Lavik G, Thamdrup B. 2008. Rates and regulation of anaerobic ammonium oxidation and denitrification in the Black Sea. *Limnol. Oceanogr.* 53:23–36. <http://dx.doi.org/10.4319/lo.2008.53.1.0023>.
  22. Kalvelage T, Jensen MM, Contreras S, Revsbech NP, Lam P, Günter M, LaRoche J, Lavik G, Kuypers MM. 2011. Oxygen sensitivity of anammox and coupled N-cycle processes in oxygen minimum zones. *PLoS One* 6:e29299. <http://dx.doi.org/10.1371/journal.pone.0029299>.
  23. Babbín AR, Keil RG, Devol AH, Ward BB. 2014. Organic matter stoichiometry, flux, and oxygen control nitrogen loss in the ocean. *Science* 344:406–408. <http://dx.doi.org/10.1126/science.1248364>.
  24. Kuypers MM, Lavik G, Woeckel D, Schmid M, Fuchs BM, Amann R, Jørgensen BB, Jetten MS. 2005. Massive nitrogen loss from the Benguela Upwelling system through anaerobic ammonium oxidation. *Proc. Natl. Acad. Sci. U. S. A.* 102:6478–6483. <http://dx.doi.org/10.1073/pnas.0502088102>.
  25. Robertson LA, Dalsgaard T, Revsbech NP, Kuenen JG. 1995. Confirmation of aerobic denitrification in batch cultures, using gas-chromatography and N-15 mass-spectrometry. *FEMS Microbiol. Ecol.* 18:113–119. <http://dx.doi.org/10.1111/j.1574-6941.1995.tb00168.x>.
  26. Paulmier A, Ruiz-Pino D. 2009. Oxygen minimum zones (OMZs) in the modern ocean. *Prog. Oceanogr.* 80:113–128. <http://dx.doi.org/10.1016/j.pocean.2008.08.001>.
  27. Dalsgaard T, Canfield DE, Petersen J, Thamdrup B, Acuña-González J. 2003. N<sub>2</sub> production by the anammox reaction in the anoxic water column of Golfo Dulce, Costa Rica. *Nature* 422:606–608. <http://dx.doi.org/10.1038/nature01526>.
  28. Stewart FJ, Ulloa O, DeLong EF. 2012. Microbial metatranscriptomics in a permanent marine oxygen minimum zone. *Environ. Microbiol.* 14: 23–40. <http://dx.doi.org/10.1111/j.1462-2920.2010.02400.x>.
  29. Stewart FJ. 2013. Preparation of microbial community cDNA for metatranscriptomic analysis in marine plankton. *Methods Enzymol.* 531: 187–218.
  30. Feike J, Jürgens K, Hollibaugh JT, Krüger S, Jost G, Labrenz M. 2012. Measuring unbiased metatranscriptomics in suboxic waters of the central Baltic Sea using a new *in situ* fixation system. *ISME J.* 6:461–470. <http://dx.doi.org/10.1038/ismej.2011.94>.
  31. De Brabandere L, Thamdrup B, Revsbech NP, Foadi R. 2012. A critical assessment of the occurrence and extend of oxygen contamination during anaerobic incubations utilizing commercially available vials. *J. Microbiol. Methods* 88:147–154. <http://dx.doi.org/10.1016/j.mimet.2011.11.001>.
  32. Stewart FJ, Dalsgaard T, Young CR, Thamdrup B, Revsbech NP, Ulloa O, Canfield DE, DeLong EF. 2012. Experimental incubations elicit profound changes in community transcription in OMZ bacterioplankton. *PLoS One* 7:e37118. <http://dx.doi.org/10.1371/journal.pone.0037118>.
  33. Raghoebarsing AA, Pol A, van de Pas-Schoonen KT, Smolders AJ, Ettwig KF, Rijpstra WI, Schouten S, Damsté JS, Op den Camp HJ, Jetten MS, Strous M. 2006. A microbial consortium couples anaerobic methane oxidation to denitrification. *Nature* 440:918–921. <http://dx.doi.org/10.1038/nature04617>.
  34. Ettwig KF, Butler MK, Le Paslier D, Pelletier E, Mangenot S, Kuypers MM, Schreiber F, Dutilh BE, Zedelius J, de Beer D, Gloerich J, Wessels HJ, van Alen T, Luesken F, Wu ML, van de Pas-Schoonen KT, Op den Camp HJ, Janssen-Megens EM, Francoijs KJ, Stunnenberg H, Weissenbach J, Jetten MS, Strous M. 2010. Nitrite-driven anaerobic methane oxidation by oxygenic bacteria. *Nature* 464:543–548. <http://dx.doi.org/10.1038/nature08883>.
  35. Strous M, Pelletier E, Mangenot S, Rattei T, Lehner A, Taylor MW, Horn M, Daims H, Bartol-Mavel D, Wincker P, Barbe V, Fonknechten N, Vallenet D, Seguren B, Schenowitz-Truong C, Médigue C, Collingro A, Snel B, Dutilh BE, Op den Camp HJ, van der Drift C, Cirpus I, van de Pas-Schoonen KT, Harhangi HR, van Niftrik L, Schmid M, Keltjens J, van de Vossenberg J, Kartal B, Meier H, Frishman D, Huynen MA, Mewes HW, Weissenbach J, Jetten MS, Wagner M, Le Paslier D. 2006. Deciphering the evolution and metabolism of an anammox bacterium from a community genome. *Nature* 440:790–794. <http://dx.doi.org/10.1038/nature04647>.
  36. van de Vossenberg J, Woeckel D, Maalcke WJ, Wessels HJ, Dutilh BE, Kartal B, Janssen-Megens EM, Roeselers G, Yan J, Speth D, Gloerich J, Geerts W, van der Biezen E, Pluk W, Francoijs KJ, Russ L, Lam P, Malfatti SA, Tringe SG, Haaij SC, Op den Camp HJ, Stunnenberg HG, Amann R, Kuypers MM, Jetten MS. 2013. The metagenome of the marine anammox bacterium “*Candidatus Scalindua profunda*” illustrates the versatility of this globally important nitrogen cycle bacterium. *Environ. Microbiol.* 15:1275–1289. <http://dx.doi.org/10.1111/j.1462-2920.2012.02774.x>.
  37. Baumann B, Snozzi M, Zehnder AJ, Van Der Meer JR. 1996. Dynamics of denitrification activity of *Paracoccus denitrificans* in continuous culture during aerobic-anaerobic changes. *J. Bacteriol.* 178:4367–4374.
  38. Baumann B, Snozzi M, VanderMeer JR, Zehnder AJB. 1997. Development of stable denitrifying cultures during repeated aerobic-anaerobic transient periods. *Water Res.* 31:1947–1954. [http://dx.doi.org/10.1016/S0043-1354\(97\)00053-5](http://dx.doi.org/10.1016/S0043-1354(97)00053-5).
  39. De Brabandere L, Canfield DE, Dalsgaard T, Friederich GE, Revsbech NP, Ulloa O, Thamdrup B. 2014. Vertical partitioning of nitrogen-loss processes across the oxic-anoxic interface of an oceanic oxygen minimum zone. *Environ. Microbiol.* 16:3041–3054. <http://dx.doi.org/10.1111/1462-2920.12255>.
  40. Thamdrup B, Dalsgaard T, Jensen MM, Ulloa O, Farias L, Escobedo R. 2006. Anaerobic ammonium oxidation in the oxygen-deficient waters off northern Chile. *Limnol. Oceanogr.* 51:2145–2156. <http://dx.doi.org/10.4319/lo.2006.51.5.2145>.
  41. Härtig E, Zumft WG. 1999. Kinetics of nirS expression (cytochrome *cd*<sub>1</sub> nitrite reductase) in *Pseudomonas stutzeri* during the transition from aerobic respiration to denitrification: Evidence for a denitrification-specific nitrate- and nitrite-responsive regulatory system. *J. Bacteriol.* 181: 161–166.
  42. Kofoed MV, Nielsen DA, Revsbech NP, Schramm A. 2012. Fluorescence *in situ* hybridization (FISH) detection of nitrite reductase transcripts (nirS mRNA) in *Pseudomonas stutzeri* biofilms relative to a microscale oxygen gradient. *Syst. Appl. Microbiol.* 35:513–517. <http://dx.doi.org/10.1016/j.syapm.2011.12.001>.
  43. Bergaust L, Shapleigh J, Frostegård A, Bakken L. 2008. Transcription and activities of NO<sub>x</sub> reductases in *Agrobacterium tumefaciens*: the influence of nitrate, nitrite and oxygen availability. *Environ. Microbiol.* 10: 3070–3081. <http://dx.doi.org/10.1111/j.1462-2920.2007.01557.x>.
  44. Shapleigh JP. 2011. Oxygen control of nitrogen oxide respiration, focusing on  $\alpha$ -proteobacteria. *Biochem. Soc. Trans.* 39:179–183. <http://dx.doi.org/10.1042/BST0390179>.
  45. Jetten MS, van Niftrik L, Strous M, Kartal B, Keltjens JT, Op den Camp HJ. 2009. Biochemistry and molecular biology of anammox bacteria. *Crit. Rev. Biochem. Mol. Biol.* 44:65–84.
  46. Sohaskey CD, Wayne LG. 2003. Role of narK2X and narGHJI in hypoxic upregulation of nitrate reduction by *Mycobacterium tuberculosis*. *J. Bacteriol.* 185:7247–7256. <http://dx.doi.org/10.1128/JB.185.24.7247-7256.2003>.
  47. Sohaskey CD. 2005. Regulation of nitrate reductase activity in *Mycobacterium tuberculosis* by oxygen and nitric oxide. *Microbiology* 151: 3803–3810. <http://dx.doi.org/10.1099/mic.0.28263-0>.
  48. Asanuma N, Iwamoto M, Yoshii T, Hino T. 2004. Molecular characterization and transcriptional regulation of nitrate reductase in a ruminal bacterium, *Selenomonas ruminantium*. *J. Gen. Appl. Microbiol.* 50: 55–63. <http://dx.doi.org/10.2323/jgam.50.55>.
  49. Körner H, Zumft WG. 1989. Expression of denitrification enzymes in response to the dissolved oxygen level and respiratory substrate in continuous culture of *Pseudomonas stutzeri*. *Appl. Environ. Microbiol.* 55: 1670–1676.
  50. Coyne MS, Tiedje JM. 1990. Induction of denitrifying enzymes in oxygen-limited *Achromobacter cycloclastes* continuous culture. *FEMS Microbiol. Ecol.* 73:263–270. <http://dx.doi.org/10.1111/j.1574-6968.1990.tb03949.x>.
  51. McKenney DJ, Drury CF, Findlay WI, Mutus B, McDonnell T, Gajda C. 1994. Kinetics of denitrification by *Pseudomonas fluorescens*—oxygen effects. *Soil Biol. Biochem.* 26:901–908. [http://dx.doi.org/10.1016/0038-0717\(94\)90306-9](http://dx.doi.org/10.1016/0038-0717(94)90306-9).

52. Stewart FJ. 2011. Dissimilatory sulfur cycling in oxygen minimum zones: an emerging metagenomics perspective. *Biochem. Soc. Trans.* 39: 1859–1863. <http://dx.doi.org/10.1042/BST20110708>.
53. Stevens H, Ulloa O. 2008. Bacterial diversity in the oxygen minimum zone of the eastern tropical South Pacific. *Environ. Microbiol.* 10: 1244–1259. <http://dx.doi.org/10.1111/j.1462-2920.2007.01539.x>.
54. Dugdale RC, Goering JJ, Barber RT, Smith RL, Packard TT. 1977. Denitrification and hydrogen-sulfide in Peru upwelling region during 1976. *Deep Sea Res.* 24:601–608. [http://dx.doi.org/10.1016/0146-6291\(77\)90530-6](http://dx.doi.org/10.1016/0146-6291(77)90530-6).
55. Schunck H, Lavik G, Desai DK, Grosskopf T, Kalvelage T, Loscher CR, Paulmier A, Contreras S, Siegel H, Holtappels M, Rosenstiel P, Schilhabel MB, Graco M, Schmitz RA, Kuypers MM, Laroche J. 2013. Giant hydrogen sulfide plume in the oxygen minimum zone off Peru supports chemolithoautotrophy. *PLoS One* 8:e68661. <http://dx.doi.org/10.1371/journal.pone.0068661>.
56. Lavik G, Stührmann T, Brüchert V, Van der Plas A, Mohrholz V, Lam P, Mussmann M, Fuchs BM, Amann R, Lass U, Kuypers MM. 2009. Detoxification of sulphidic African shelf waters by blooming chemolithotrophs. *Nature* 457:581–584. <http://dx.doi.org/10.1038/nature07588>.
57. Sørensen J, Tiedje JM, Firestone RB. 1980. Inhibition by sulfide of nitric and nitrous oxide reduction by denitrifying *Pseudomonas fluorescens*. *Appl. Environ. Microbiol.* 39:105–108.
58. Dalsgaard T, De Brabandere L, Hall POJ. 2013. Denitrification in the water column of the central Baltic Sea. *Geochim. Cosmochim. Acta* 106: 247–260. <http://dx.doi.org/10.1016/j.gca.2012.12.038>.
59. Braman RS, Hendrix SA. 1989. Nanogram nitrite and nitrate determination in environmental and biological materials by vanadium (III) reduction with chemiluminescence detection. *Anal. Chem.* 61:2715–2718. <http://dx.doi.org/10.1021/ac00199a007>.
60. Grasshoff K. 1983. Determination of nitrite, p 1392715–142. In Grasshoff K, Ehrhardt M, Kremling K (ed), *Methods of seawater analysis*, 2nd ed. Verlag Chemie GmbH, Weinheim, Germany.
61. Holmes RM, Aminot A, Kerouel R, Hooker BA, Peterson BJ. 1999. A simple and precise method for measuring ammonium in marine and freshwater ecosystems. *Can. J. Fish. Aquat. Sci.* 56:1801–1808. <http://dx.doi.org/10.1139/f99-128>.
62. Cline JD. 1969. Spectrophotometric determination of hydrogen sulfide in natural waters. *Limnol. Oceanogr.* 14:454–458. <http://dx.doi.org/10.4319/lo.1969.14.3.0454>.
63. Thamdrup B, Dalsgaard T. 2002. Production of N<sub>2</sub> through anaerobic ammonium oxidation coupled to nitrate reduction in marine sediments. *Appl. Environ. Microbiol.* 68:1312–1318. <http://dx.doi.org/10.1128/AEM.68.3.1312-1318.2002>.
64. Jensen MM, Thamdrup B, Dalsgaard T. 2007. Effects of specific inhibitors on anammox and denitrification in marine sediments. *Appl. Environ. Microbiol.* 73:3151–3158. <http://dx.doi.org/10.1128/AEM.01898-06>.
65. Stewart FJ, Ottesen EA, DeLong EF. 2010. Development and quantitative analyses of a universal rRNA-subtraction protocol for microbial metatranscriptomics. *ISME J.* 4:896–907. <http://dx.doi.org/10.1038/ismej.2010.18>.
66. Frias-Lopez J, Shi Y, Tyson GW, Coleman ML, Schuster SC, Chisholm SW, DeLong EF. 2008. Microbial community gene expression in ocean surface waters. *Proc. Natl. Acad. Sci. U. S. A.* 105:3805–3810. <http://dx.doi.org/10.1073/pnas.0708897105>.
67. Li W, Godzik A. 2006. Cd-hit: a fast program for clustering and comparing large sets of protein or nucleotide sequences. *Bioinformatics* 22: 1658–1659. <http://dx.doi.org/10.1093/bioinformatics/btl158>.
68. Ganesh S, Parris DJ, DeLong EF, Stewart FJ. 2014. Metagenomic analysis of size-fractionated picoplankton in a marine oxygen minimum zone. *ISME J.* 8:187–211. <http://dx.doi.org/10.1038/ismej.2013.144>.
69. Huson DH, Mitra S, Ruscheweyh HJ, Weber N, Schuster SC. 2011. Integrative analysis of environmental sequences using MEGAN4. *Genome Res.* 21:1552–1560. <http://dx.doi.org/10.1101/gr.120618.111>.
70. Zumft WG. 1997. Cell biology and molecular basis of denitrification. *Microbiol. Mol. Biol. Rev.* 61:533–616.
71. Vajrala N, Martens-Habbena W, Sayavedra-Soto LA, Schauer A, Bottomley PJ, Stahl DA, Arp DJ. 2013. Hydroxylamine as an intermediate in ammonia oxidation by globally abundant marine archaea. *Proc. Natl. Acad. Sci. U. S. A.* 110:1006–1011. <http://dx.doi.org/10.1073/pnas.1212277109>.